Transparent Electro-Optic Ceramics and Devices

H. Jiang*, Y.K. Zou, Q. Chen, K.K. Li, R. Zhang, and Y. Wang
Boston Applied Technologies, Incorporated, Woburn, MA 01801, USA

ABSTRACT

This paper summarizes the material synthesis and properties of transparent electro-optic ceramics, namely OptoCeramic®, including PLZT and PMN-PT. Material structure, dielectric, optical and electro-optic properties are discussed. OptoCeramic materials feature in high E-O effect, low optical loss, broad transmission wavelength range, ceramic ruggedness, and low cost. A variety of devices made from OptoCeramic materials are discussed, including variable optical attenuators, polarization controllers, sinusoidal filters, dynamic gain flattening filters, tunable optical filters, and Q-switches.

Keywords: OptoCeramic®, electro-optic, transparent ceramics, polycrystalline, high EO effect, fiber optic devices

1. INTRODUCTION

High performance solid electro-optic oxides are the only class of materials possessing both large and fast electro-optic effects. $LiNbO_3$ single crystals are the industry benchmark of electro-optic material used in telecommunications. However, some drawbacks of $LiNbO_3$ crystal, such as low electro-optic (EO) effect and high temperature dependency, made it difficult for widespread applications. OptoCeramic® is a family of transparent electro-optic ceramic materials, it features high EO effect, good transparency, ceramic ruggedness, and low cost. PLZT,[1] one of the OptoCeramic® family members, has much higher EO effect than that of $LiNbO_3$, however, its significant field induced and polarization dependent scattering losses and high hysteresis made it problematic in controlling dynamic devices. The newly developed modified $Pb(Mg_{1/3}Nb_{2/3})O_3$-$PbTiO_3$ (PMN-PT)[2] OptoCeramic® has greatly alleviated the aforementioned issues. PMN-PT is in a class of materials called relaxors, which have an isotropic minimum energy stable structure and upon applying an electric field can be relatively easily distorted, producing birefringence thus exhibiting the E-O effect. Its EO effect is about 2-5 times higher than that of PLZT and nearly 100 times than $LiNbO_3$ at room temperature. To reach the same index change (or phase shift), the applied voltage on PMN-PT is much lower than that on PLZT and $LiNbO_3$. The hysteresis of PMN-PT ceramic is also significantly reduced over the temperature range from 0° to 70°C. Unlike crystal materials, polycrystalline electro-optic ceramic is much easier to make by the mature hot-pressing technique at low cost. The remarkably good transparency over a wide wavelength range of 500nm-7000nm makes PMN-PT OptoCeramic® best suited for almost all the visible to mid IR optical applications. The isotropic feature of OptoCeramic® materials is ideally suited for polarization independent device fabrication. Furthermore, the electron and ion movement responsible for the EO effect are much faster than that of molecular movement in liquid crystal materials. Nanoseconds modulation has been demonstrated in OptoCeramic® materials. In this paper, we report the material fabrication process and properties of PMN-PT OptoCeramic and compare it with PLZT. A variety of devices have been developed using OptoCeramic®

* hjiang@bostonati.com; phone 781-935-2800; fax 781-935-2860; www.bostonati.com

materials, including variable optical attenuator, polarization controller, tunable optical filter, dynamic gain flattening filter, etc. OptoCeramic® device related results are described in section 3.

2. ELECTRO-OPTIC CERAMIC MATERIALS

2.1. OptoCeramic materials

OptoCeramics is a family of transparent oxide electro optic ceramic materials. Their crystallography structure is perovskite type with the formulation of ABO_3. The typical representatives of this family are $Pb_{1-x}La_x(Zr_yTi_{1-y})_{1-x/4}O_3$ (PLZT), $Pb(Mg_{1/3}Nb_{2/3})O_3$-$PbTiO_3$ (PMN-PT), and $Pb(Zn_{1/3}Nb_{2/3})O_3$-$PbTiO_3$ (PZN-PT).[3] The PLZT formula assumes that La substitutes for Pb^{2+} in the A-site and the B-site vacancies are created for electrical balance. The PLZT composition is conventionally abbreviated as x/y/1-y, by which a PLZT 9/65/35 composition means a La concentration of 9 at.% with a Zr/Ti ratio of 65 to 35. To achieve the best transparency and electro-optic coefficient, some elements, such as Ba and/or La, are usually added to the solid solutions of PMN-PT and PZN-PT. Shown in Figure 1 are the phase diagrams of PLZT[4] and PMN-PT.[5] Electro-optic compositions in the PLZT phase diagram are generally divided into three application areas: quadratic, memory, and linear. The quadratic materials are compositionally located along the phase boundary separating the ferroelectric and paraelectric phases, principally in the crosshatched area. Memory compositions having stable, electrically switchable optical states are largely located in the ferroelectric (FE) rhombohedral phase region, and the linear materials possess nonswitching, linear electrooptic effects are confined to the area encompassing the tetragonal phase. A less studied composition region is the antiferroelectric (AFE) phase near the $PbZrO_3$ side of the phase diagram. Although a large range of composition we have investigated, the compositions of materials we report in this paper are located near the quadratic region.

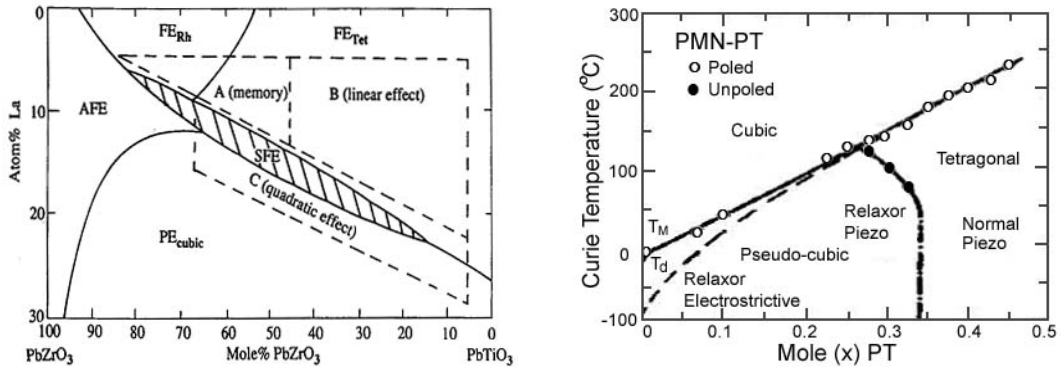

(a) (b)

Figure 1. (a) Phase diagram of PLZT at room temperature,[4] (b) Temperature dependent phase diagram of PMN-PT.[5]

2.1.1. Fabrication process

A uniaxial hot-press system (Thermal Technology, Model HP52-0914-SC) was used for the ceramic fabrication. The system is fully computer controlled and is capable for making 4"-diameter high quality ceramic materials. Bayonet-type silicon carbide heating elements were housed in a controlled atmosphere/vacuum zone to provide a maximum temperature up to 1500°C. A motor driven hydraulic force system can provide a force up to 25 tons. A Pt-Rh (type B) thermocouple was used as the temperature sensing element together with a digital

microprocessor-based automatic temperature controller.

Ferroelectric ceramics are traditionally made from powders formulated from individual oxides; however, for electro-optic materials powders made from a chemical coprecipitation technique is more appropriate. Understandably, the electro-optic ceramics require a higher purity, more homogeneous, and high-reactivity powder than other non-optic materials because inhomogeneities is much more sensitive optically than electrically.

In the CP process for PLZT, high-purity liquid organometallics (tetrabutyl zirconate and tetrabutyl titanate) are first premixed with lead oxide in a high-speed blender and then precipitated by adding the lanthanum acetate, water-soluble solution while blending. The resulting slurry, consisting of a finely divided suspension of mixed oxides and hydroxides in an alcohol-water solution, is dried to completion at approximately 80°C. Subsequent steps in the process involve (1) calcining the powder at 500°C for 16 hrs, (2) wet milling the powder for several hours to promote additional homogeneity, (3) drying without binder, (4) cold pressing the powder. Up to now, the cold pressed preform is ready for hot-pressing. For PMN-PT or PZN-PT, all the procedures are the same as those for PLZT except the starting materials are the corresponding organometallics.

Uniaxial hot-press is used to fabricate optical-quality ceramic materials. The preformed powder is hot pressed in a SiC mold and surrounded by refractory grain (magnesia or zirconia) to prevent reactions between the growing and surrounding materials at high temperature. During the heating portion of the hot-press cycle, the slug is evacuated and back-filled with oxygen. Typical hot-pressing conditions are 1200-1300°C for more than 10 hrs at 2000 psi. After hot pressing, the slug is extracted from the mold and polished for optical evaluation. Shown in Figure 2 are examples of the hot-pressed OptoCeramics in slug and wafer form.

Figure 2. Hot-pressed OptoCeramic slugs and wafers.

The two most critical steps in the fabrication of these ceramic materials are powder preparation and firing, and of these, the first is predominant. Although one can readily determine many measurable characteristics of the powders, such as particle size, surface area, composition, crystalline structure, and morphology, powder reactivity (the tendency of particles to inter-diffuse and coalesce at some elevated temperature) is the most important one, but is still the least understood. In fact, a primary objective of the various chemical preparation techniques is to increase powder reactivity, thereby achieving full density (zero porosity) and maximum chemical homogeneity.

2.1.2. Material properties

The PLZT and PMN-PT materials made from hot-pressing are polycrystalline that can be seen from the x-ray diffraction patterns shown in Figure 3. The only crystalline phase is the perovskite structure with no secondary impurity phase detected. This is a necessary requirement in achieving optical grade ferroelectrics. PMN-PT has almost identical x-ray diffraction patterns as PLZT except all the peaks shifted toward the larger diffraction angle, which indicated that PMN-PT had slightly smaller lattice constants than those of PLZT. The polycrystalline nature makes the OptoCeramic materials homogenous in structure, and thus polarization independent. This feature is

especially convenience in device design and processing since there would be no need to consider the crystalline orientation that is usually troublesome in single crystal materials.

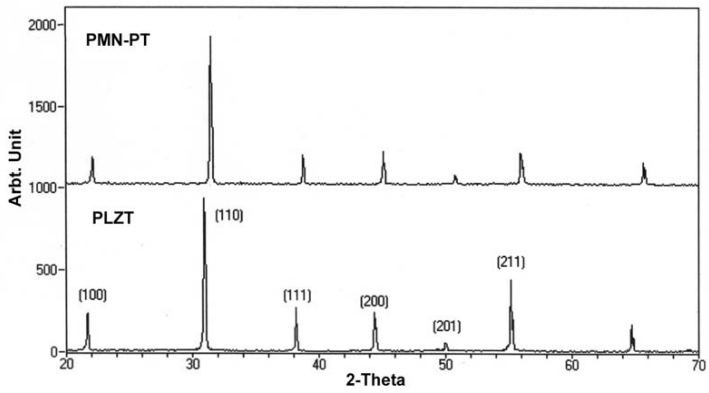

Figure 3. X-ray diffraction curves of PLZT and PMN-PT transparent ceramic materials.

The electric hysteresis loop of the hot-pressed PLZT (9.5/65/35) and PMN-PT ceramics are shown in Figure 4(a) and Figure 4(b), respectively. These data were measured at a relatively low (about half) electric field than that conventionally used to measure PLZTs. It can be seen that PMN-PT is much more active and therefore achieves saturation in polarization at this low field while PLZT is not. Since electrical polarization is closely related to the electro-optical properties, this means that PMN-PT has a high EO coefficient. Also to be noted is the almost lack of any significant hysteresis, or difference between increasing and decreasing the electrical driving voltage, in the PMN-PT materials. This behavior is known and typical for this class of ferroelectric material called relaxor ferroelectrics. Lack of hysteresis is an important merit in any device applications.

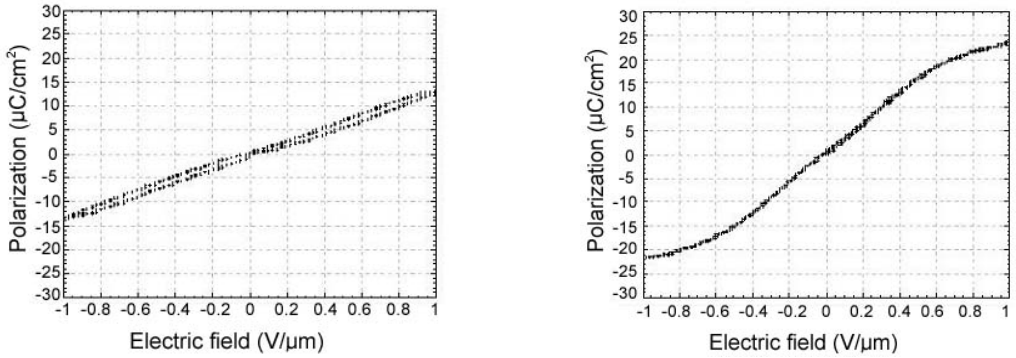

Figure 4. Electric hysteresis properties of PLZT (a) and PMN-PT (b) ceramic materials.

The dielectric and optic properties of transparent electro-optic ceramics are closely dependent on the grain size. The grain size of the ceramics can be controlled by varying the hot-pressing temperature and time. Shown in Figure 5 are the microimages of PLZT wafers prepared through thermal etching. Grains can be clearly viewed and precisely measured. Table 1 lists various electrical and electro-optic properties of PMN-PT and PLZT with different grain sizes.

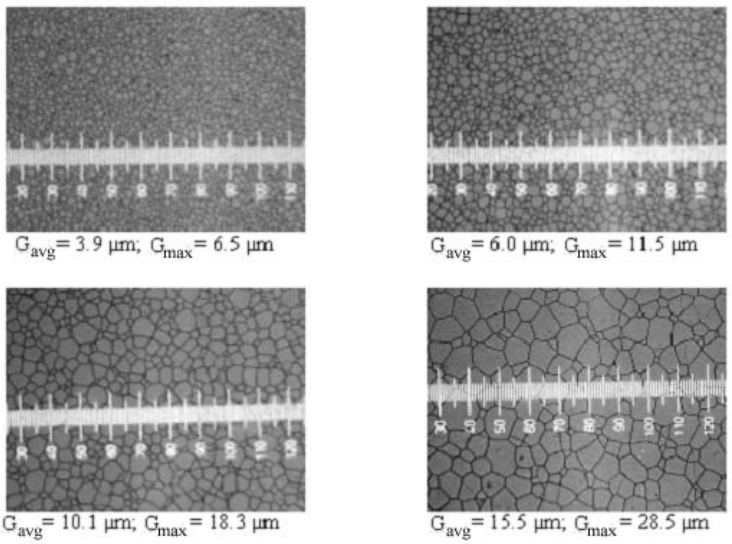

Figure 5. OptoCeramic samples with different grain sizes.

Table 1. Various dielectric and electro-optic properties of PMN-PT and PLZT with controlled grain sizes.

Material	PMN-PT	PLZT			
Firing Temperature (°C)	1200-1300	1300	1250	1150	1050
Grain Size (µm)	3-7	16	10	5	4
Dielectric Constant @ 1 kHz	20,000-25,000	-	4,626	4,579	4,377
Dielectric Loss (%) @ 1 kHz	3-5	-	3.7	3.5	3.5
E_π (V/µm) (optical path is 1.4mm)	0.175-0.28	-	0.55	0.59	0.59

Figure 6 illustrate the dielectric constants of PLZT and PMN-PT as functions of temperature. When the La concentration in the PLZT (Zr/Ti ratio is 65/35) increases from 9 to 10, as shown in Figure 6(a), the peak dielectric constant decreases from 9450 to 8000 and the peak temperature decreases from 70°C to 53°C. In normal ferroelectrics, the Curie temperature is defined as the temperature where the material changes from ferroelectric to paraelectric phase, or where dielectric constant peaks. Shown in Figure 6(b) are the curves of dielectric constant and dielectric loss versus temperature for a modified PMN-PT at different frequencies (from 0.1 to 100 KHz). The dielectric loss data refers to the axis at the right side of the graph. PMN-PT material has higher dielectric constant at lower frequency and decreases monolithically when the measurement frequency increases. The dielectric constant of PMN-PT is significantly (2-3 times) higher than that of PLZT.

OptoCeramic materials have excellent transparency over a wide range of wavelength band, from visible to middle IR. Shown in Figure 7 is the optical transmission spectrum of a PMN-PT wafer with a thickness of 1.45 mm from 300 to 1800 nm. A spectrometer (Shimadzu UV-3101PC) was used for the measurement. Since the refractive index of the material ranges from 2.3 to 2.5 in the wavelength band of measurement, reflection loss exists at the air/ceramic interface. When measured on AR coated PMN-PT wafers, less than 0.025 dB/mm at wavelength of 1.55 µm was obtained. The inset of Figure 7 is a redrawing of the transmission curve of a PLZT wafer measured in 300-1800 nm and 2 -8.3 µm. The latter spectrum was measured with a Perkin-Elmer 983 Infrared

Spectrophotometer. Although we did not measure the whole wavelength range as shown in the inset of Figure 7 for PMN-PT, the transmissions at several selective wavelengths we measured match or are slightly better than those of PLZT.

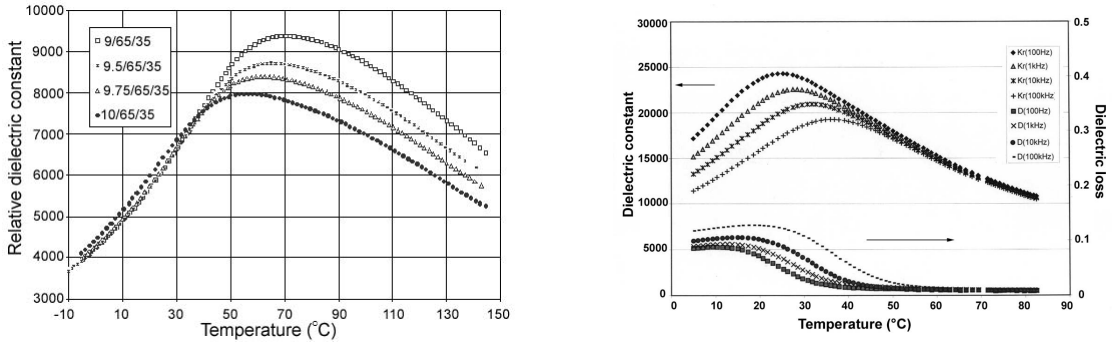

(a) (b)

Figure 6. Dielectric constants of PLZT and PMN-PT as functions of temperature. (a) PLZT, (b) PMN-PT.

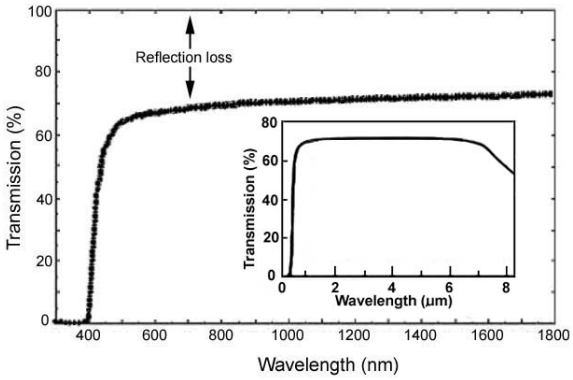

Figure 7. Optical transmission spectrum of a PMN-PT wafer with a thickness of 1.45 mm. The inset is a redrawing of the spectrum of a PLZT wafer.

PMN-PT is a quadratic Kerr EO material. Shown in Figure 8 is the phase retardation (shift) of a PMN-PT and a PLZT sample as a function of electric fields at wavelength of 1550 nm. The phase retardation (Γ) follows

$$\Gamma = \frac{\pi t n^3 R E^2}{\lambda}, \quad (1)$$

where R is the EO coefficient, n the optical refractive index, λ the wavelength, and t the path length light travels in the material. From Equation (1), EO coefficients of 13.3 $x10^{-16}$ m^2/V^2 and $2.8x10^{-16}$ m^2/V^2 can been deduced for PMN-PT and PLZT at room temperature, respectively. The highest EO coefficient we have achieved in PMN-PT is 28 $x10^{-16}$ m^2/V^2.

Comparing to PLZT, PMN-PT has lower field induced optical loss, or so-called activation loss, as shown in Figure 9. Activation loss will degrade the device performance when applied voltage is close to or over the half-wave voltage, V_π.

One important property of OptoCeramic materials is the fast response speed. The electronic and ionic

movements responsible for the E-O effect are much faster than that of molecular movement in liquid crystal materials. Sub-microsecond speed can be realized in devices made from OptoCeramic materials. Shown in Figure 10(a) is the switching speed of a test structure made from OptoCeramic thin film material, which is about 10 ns. Similar measurement on bulk materials showed less than 100 ns switching (Figure 10(b)). It is important to point out that the response speed measurement is highly dictated by the electronic driving circuit; therefore, the measured speed may not represent the intrinsic speed of the material.

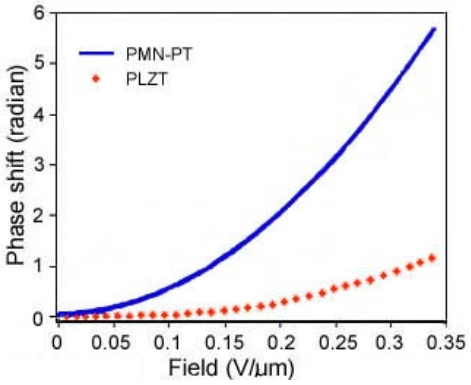

Figure 8. Measured retardance (phase shift) vs. applied field of PMN-PT at wavelength of 1.55μm.

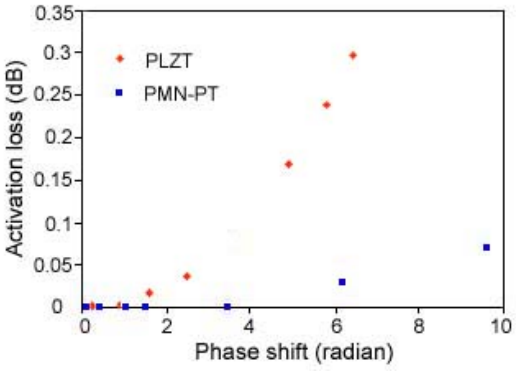

Figure 9. Activation loss of PLZT and PMN-PT.

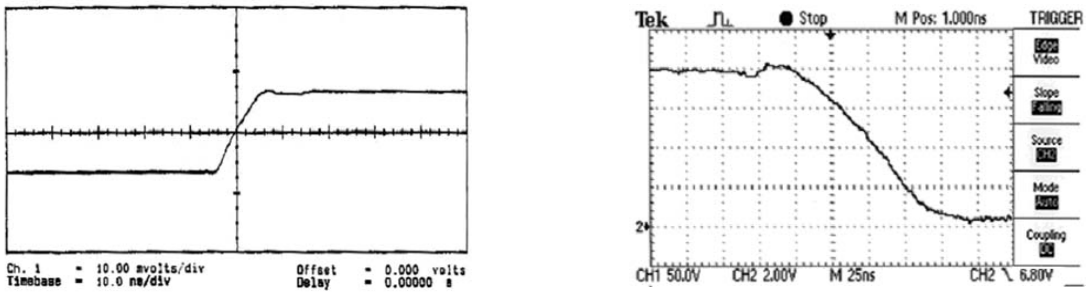

(a) (b)

Figure 10. High speed switching of test structures made from OptoCeramic materials. (a) OptoCeramic thin film, 10 ns; (b) OptoCeramic bulk material, 100 ns.

3. DEVICES MADE FROM OPTOCERAMIC MATERIALS

Dynamic photonic components are critical in controlling the network in the optical domain, especially in the dense wavelength-division multiplexing (DWDM) systems, which can dramatically improve network speed, capacity, adaptability and reliability. Optical signal can be controlled via mechanical, thermal, magnetic, and electrical approaches. Besides the mechanical method, all the other methods are based on the controlling of refractive index of the media in which lightwave propagates. By manipulating refractive index, all the optical properties, such as intensity, phase, and polarization, can be controlled by proper optical arrangement.

Thermo-optic devices take advantage of the dependence of the refractive index on material temperature. While the optical characteristics of thermo-optic devices are attractive, the response time is very slow and reliability

remains unproven. Cross-talk is another issue for integrated thermo-optic devices. Magneto-optic material is quite successfully used for passive optical isolators or latching devices. However, for dynamic device applications, magneto-optical approach is not attractive since it requires a current-driven electromagnet to adjust the magnetic field. Electro-optic approach is a convenient way by changing the index of refraction in an electro-optic (EO) material through application of an electric field. Devices made from electro-optic materials offer excellent optical specifications and high-speed operation.

The excellent optical and electro-optic properties of OptoCeramic materials, especially transparent electro-optic PMN-PT ceramics, are ideal for dynamic photonic device applications. Several types of dynamic photonic devices have been developed using OptoCeramic materials and are described in the following sections.

3.1. Variable Optical Attenuator (VOA)

Electronically controllable variable optical attenuators (VOA) play a crucial role in controlling optical signal levels throughout the network. The main network applications for VOA are: (1) Pre-emphasis. In DWDM transmission, the optical power between all channels needs to be equalized before they are combined into a single optical fiber. (2) Channel balancing. At add/drop network nodes, channel equalization is imperative because optical signals arrive independently from different points in a network. (3) Optical automatic gain control. Simultaneous attenuation of multiple wavelengths between stages in erbium-doped fiber amplifiers (EDFAs) enables tuning of amplifier gain for specific span lengths. This capability optimizes power levels throughout the transmission line and reduces spectral gain tilt induced in EDFAs by changing optical power. VOAs can be combined with other functionalities for new uses. Beyond network uses, VOA demand by instrumentation manufacturers has dramatically increased. For example, VOAs contribute to tunable laser instrumentation by maintaining constant output power during a sweep across a range of wavelengths.

High EO effect OptoCeramic (OC) materials enable the design of devices using a non-guided, free-space configuration. In our design, light travels perpendicular to the surface of OC material, enabling low insertion loss and polarization-insensitive operation. These devices are constructed in a manner similar to that of isolators, a well-understood network component. Light is introduced via an input collimator; it passes through an OC element and exits by way of an output collimator. Attenuation control is realized by adjusting the electric field within the OC element - modification of the material's refractive index changes the level of light output. A schematic of the construction as well as an Eclipse^{TM} VOA device are shown in Figure 11. This compact VOA has a footprint of only 65 mm^2 (10 x 6.5 x 6 mm, excluding the fiber protectors); therefore, they are readily been arrayed up to cover a group of channels in a straightforward fashion.

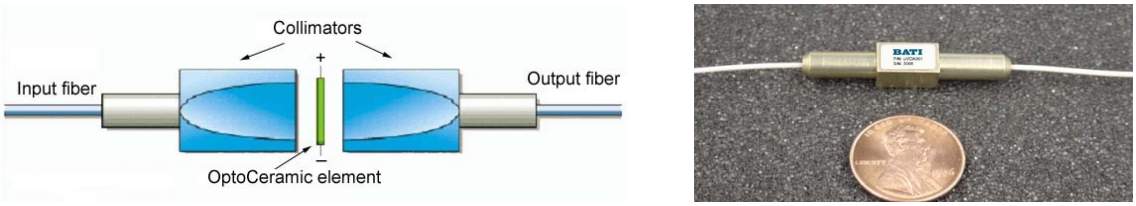

Figure 11. Schematic of the VOA construction and an Eclipse^{TM} VOA device.

Typical dynamic range of the VOAs is 25 dB and the better ones can reach 35 dB. Typical wavelength-dependent loss (WDL) and polarization-dependent loss (PDL) are 0.25 dB (0.1 dB achievable) at 15-dB attenuation, with insertion loss less than 0.6 dB (0.3 dB achievable). The fundamental response time of these VOAs is well under 1 μsec; such high speed permits the implementation of a real-time close-loop control system, which has the benefits of precise attenuation settings based on real-time light intensities and very small temperature dependence. Table 2 summarizes the performance parameters of VOAs made from OptoCeramics. The intrinsic fast speed of these VOAs makes it possible for modulation at sub-MHz range, which is suitable for channel supervising. Figure 12 shows the optical modulation of a VOA at 1 MHz. With the advent of high-speed VOA technology, network designers are now able to increase the flow of control information between network nodes without requiring the expense and high insertion loss involved in optical-signal de-multiplexing. By using a VOA that has an intrinsically fast material response speed, both signal level and modulation functionalities can be implemented without increasing component count.

Table 2. Summary of the VOA performance.

Attributes	Typical	Achieved
Insertion loss (IL)	≤ 0.6 dB	≤ 0.3dB
Dynamic Range	≥ 25 dB	≥ 35 dB
WDL @ 15 dB	≤ 0.25 dB	
PDL @ 1550nm & 15dB	≤ 0.25 dB	0.1 dB
Response Time	< 30 μs	<1 μs
Input optical power	500 mW	2.7W
Return loss	≥ 55 dB	
Operating temp. range	0°C to 70°C	
Storage temperature range	-40°C to 85°C	
Dimensions	10×6.5×6 mm	

In telecommunications systems, device reliability is paramount. The combination of simple micro-optic design and ceramic ruggedness of the OptoCeramic materials provide excellent reliability. The VOAs were fully tested according to Telcordia 910, 1209 and 1221 protocols with excellent results. For example, units subjected to 85°C and 85% relative humidity have survived more than 1,000 hours with <0.15 dB shift in insertion loss. Similarly, almost no shift in insertion loss was measured following 100 cycles of -40°C to +70°C temperature cycling.

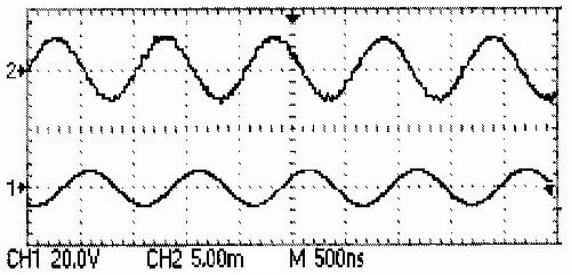

Figure 12. Optical modulation of a VOA at 1 MHz.

3.2. Polarization Controller (PC)

Light is an electromagnetic wave whose electric and magnetic fields components are orthogonal to each other and to the direction of light propagation. In other words, light is a polarized electromagnetic field. At any given instant it has distinct orientation in space and its propagation through media depends on the polarization direction. Polarization related impairments, such as polarization-dependent loss (PDL) and polarization mode dispersion (PMD), have become the major obstacles to the increased transmission rates in DWDM systems. The existence of PDL is the difference between the maximum and the minimum insertion losses for all possible input states of polarization (SoP), while PMD is a time delay or differential group delay (DGD) when the two polarization components travel with different speeds. At the receiving end, the delay between the arrivals of the two modes of the optical signal is interpreted as dispersion, which makes it difficult or impossible to interpret the optical signal. PDL may weaken signal strength while PMD may cause signal bit errors, especially when bandwidth is high.

Therefore, polarization management is a major task in controlling optical communication systems. A dynamic polarization controller is identified as the most important element for overcoming polarization related impairments.

Two dynamic retardation plates (also called retarders) placed 45º with respect to each other would be capable of changing the input SoP to any polarizations; one adjusts the polarization component along the longitude direction while another along the latitude direction on the Poincare sphere.[6] If a SoP is parallel or perpendicular to the fast (or slow) axis of the plate, such plate would have no effect on the SoP. However, when two plates are placed 45º with respect to each other, there would be no singularity point on the entire Poincare sphere since there is no circumstance that the incoming SoP would simultaneously align to the fast or slow axis of the plates. Therefore, two dynamic retarders would be sufficient to change any incoming SoP to any selectable output SoP.

OptoCeramc is ideal to play the role of dynamic retarders since its refractive index is adjustable under electric field. The large electro-optic effect of OptoCeramic material requires small electric field to achieve π phase shift, which minimizes the electric field induced scattering from the material, in turn, it produce negligible activation loss (AL). Since the major application of polarization controllers is for network impairment correction, where continuous operation is required. In circumstances when one retardation-plate reaches π phase shift, there are two options for subsequent operations: either further applying voltage beyond V_π to maintain system compensation or reducing voltage to zero and starting over again. Applying higher than V_π voltage would be at the price of higher activation loss while rewinding to zero voltage would leave the system an uncontrolled period, which is not acceptable. We add another dynamic retarder to help the rewinding process; that is, when the voltage on the rewinding plate is reduced, the extra plate would be biased up to realize a seamless and endless control.

Figure 13 shows the design of a polarization controller and an actual Acrobat^{TM} PC device. Four OptoCeramic plates are used to rotate the income SoP and they are oriented at 45°, -45° and 0°, respectively, with respect to the first plate. The functioning of the first three plates has been described in the previous paragraph; however, the additional one was added for simplifying control algorithm of system design where more than V_π voltage is required. The compact physical dimension of the PC is 22.3×11×7.8 mm^3. Table 3 lists the key parameters of the device; they are: IL ≤0.6 dB, PDL ≤0.1 dB, AL ≤0.02 dB, response time ≤30 µs. Fast speed, low PDL, low insertion loss, and low activation loss featured by the Acrobat^{TM} PC, are all critical parameters in evaluating a dynamic polarization controller. Figure 14 shows the redrawing of screen prints of a polarimetry measurement of an Acrobat^{TM} polarization controller; rotations along the longitude, latitude, and angular directions are controlled by 3 dynamic retardation plates independently. By adjusting the retardation on two plates (or 3 plates if the incoming polarization is coincidently parallel to one of the other plates), the SoP can be controlled anywhere on the Poincare Sphere. These polarization controllers can be used for polarization mode dispersion compensation, polarization scrambling, polarization multiplexing, polarization generation, and other polarization management functions.

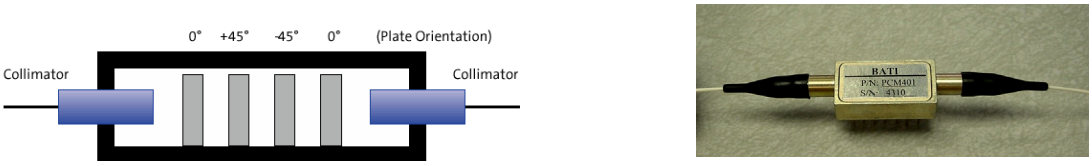

Figure 13. Schematics of a polarization controller design and an Acrobat^{TM} polarization controller.

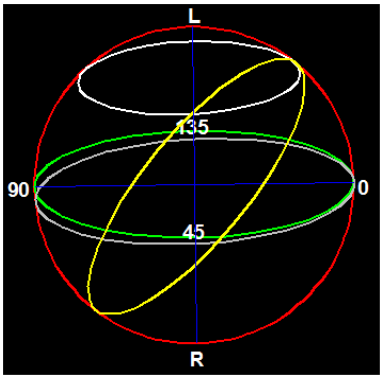

Figure 14. A screen print of the measurement of a PC.

Table 3. Key parameters of polarization controllers

Attributes	Performance
Insertion loss	≤ 0.6 dB
Polarization dependent loss	≤ 0.1 dB
Polarization mode dispersion	≤ 0.01 ps
Input power	≤ 2.7 W
Activation loss @ V_π	≤ 0.02dB
Speed	≤ 30 μs
Return loss	≥ 55 dB
Power Consumption	600 mW
Dimensions	22.3×11×7.8 mm

3.3. Variable Gain Tilt Filters (VGTF) and Dynamic Gain Flattening Filters (DGFF)

In wavelength-division-multiplexing (WDM) optical links, it is important to keep all channels at the same power levels in order to avoid signal-to-noise ratio degradation. A major cause of dynamic power variations is the power- and wavelength-dependent gain characteristics of optical amplifiers.[7] Equinox™ dynamic gain flattening filter (DGFF) is based on OptoCeramic® harmonic elements. The principle behind this is that any smooth spectrum curve can be represented by a sum of Fourier curves A_i, or raised cosines on the logarithm scale:

$$H(\omega) = \sum \log A_i(\omega) \tag{2}$$

where ω is the harmonic frequency or a set of frequencies selected to best fit the spectrum curve. The general expression of A_i is in the form of sinusoidal wave,

$$A_i(\varphi, \theta, \omega) = 1 - \frac{1}{2} \cdot \sin^2(\varphi) \cdot [1 + \cos(\theta, \omega)] \tag{3}$$

where variables φ controls the amplitude of the sinusoidal wave and θ adjusts the phase of the filter, respectively. The free spectral range (FSR) of the sinusoidal wave was determined by the harmonic frequency ω. Shown in Figure 15(a) is a schematic of Variable Gain Tilt Filters (VGTF), also called a sinusoidal filter, which consists of a pair of collimators, an amplitude tuning element, and a phase tuning element. Both the amplitude and phase tuning elements are composed from OptoCeramic® materials and corresponding passive optical components.

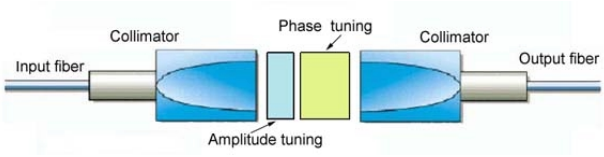

(a)

(b)

Figure 15. Schematic of a sinusoidal filter and an Equinox™ VGTF.

Shown in Figure 16 is a typical tuning curve of a sinusoidal wave filter with a FSR=24 nm. The device started with a flat spectrum and at minimum insertion loss state. Both amplitude (A) and phase (P) can be tuned individually. A and P indicate the amplitude and phase tuning positions, respectively. For simple spectra manipulating, such as changing the slope of the spectra, a sinusoidal filter with proper FSR would be sufficient.

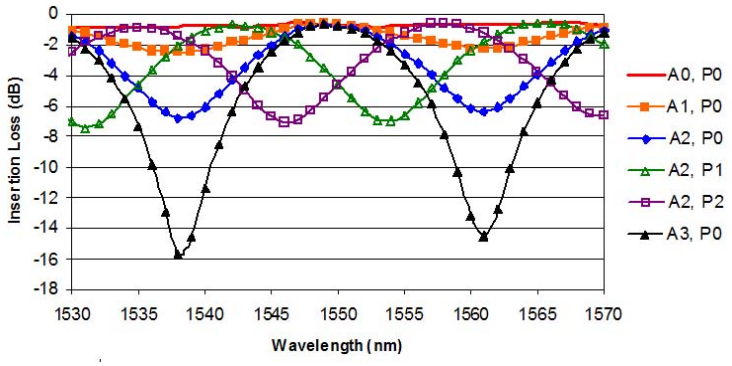

Figure 16. Measured results of a 24 nm FSR sine filter.

In order to flatten an arbitrary gain profile, multiple sinusoidal filters with different FSRs will be needed to form a dynamic gain-flattening filter (DGFF). Shown in Figure 17 is an Equinox™ DGFF consists of 5 sinusoidal filters and a VOA. Such device can also be composed from individual sinusoidal filters and VOA. Figure 18 shows the calculated flattening result of a customer target spectrum using the 5-stage DGFF. The ripple in C-band of the compensated spectrum is less than 0.5dB. Such fitting result has been verified by using an Equinox™ DGFF.

Figure 17. Equinox™ DGFF.

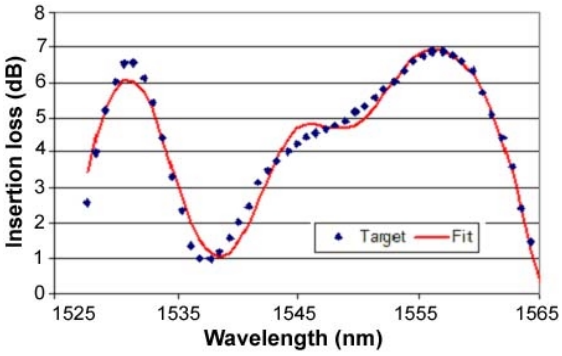

Figure 18. Fitting of a DGFF consists of 5 sine filters and a VOA.

Table 4. Key parameters of Equinox™ DGF

Attributes	Performance
IL	≤ 4dB
PDL	≤ 0.2 dB (through) ≤0.5 dB (15 dB tuning)
PMD	≤ 0.3 ps
WDL	≤ 0.3 dB
Dynamic range	> 15 dB
Response time	≤ 10 μs
Return loss	≥ 55 dB
Phase tuning	> 2π
Dimensions	105×16×9 mm

3.5. Q-switches

Q-switching is one of the most common schemes to generate pulsed laser. The name of Q-switch is originated from the working principle of Q-switched laser where the laser output is turned off by periodically spoiling the resonator quality factor, Q, with the help of a modulated absorber inside the resonator. A Q-switch? is based on loss switching. Because the pump continuously delivers constant power at all the time, energy is stored in the atoms in the form of an accumulated population difference during the off (high-loss)-times. When the losses are reduced during the on-times, the large accumulated population difference is released, generating intense short pulses of light. Among the existing Q-switches,[8,9] the electro-optic version is attractive in terms of size and

agility.[10],[11] Typical EO Q-switches are made from KDP and $LiNbO_3$. Due to the small modulation efficiency of these materials, high driving voltage (>1000 V) is usually required.

In contrast, OptoCeramics have very high EO coefficients, therefore, much lower voltage is needed for Q-switching. Low voltage is very important to achieve Q-switched lasers with high repetition rate. We have developed OptoCeramic Q-switches with driving voltage as low as 48 V, which allowed us to reach a high repetition rate over 200 KHz. In order to evaluate the Q-switch, a Q-switched diode pumped solid-state (DPSS) laser was built, as shown in Figure 19. The components used for constructing the DPSS include: a 807nm laser diode with a polarizer, a GRIN lens to focus the pump laser into the laser crystal, a plano-concave lens as the pump coupler, a Nd doped YVO_4 laser crystal, a PMN-PT Q-switch with its optical axis 45° aligned to the YVO_4 c-axis, and a 90% plane mirror as the output coupler.

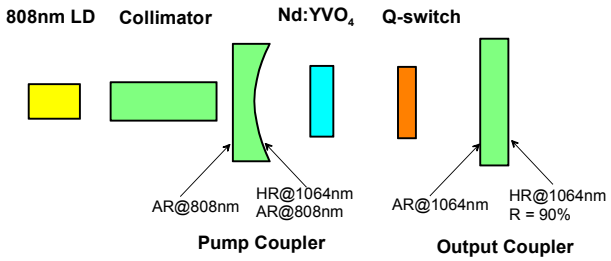

Figure 19. Configuration of a Q-switched DPSS laser.

Various laser pulses with different durations were demonstrated from 10 ns to 100 ns, with driving voltage ranging from 48 V to 106V using our driving scheme. We also found that the low repetition rate tended to give shorter pulses. Shown in Figure 20 are, respectively, the pulse width and repetition rate of a Q-switch with an aperture of 1.8×0.5 mm made from an OptoCeramic PMN-PT. This small aperture Q-switch was specially designed for fiber lasers. Other lager apertures Q-switches have also been developed for free space lasers.

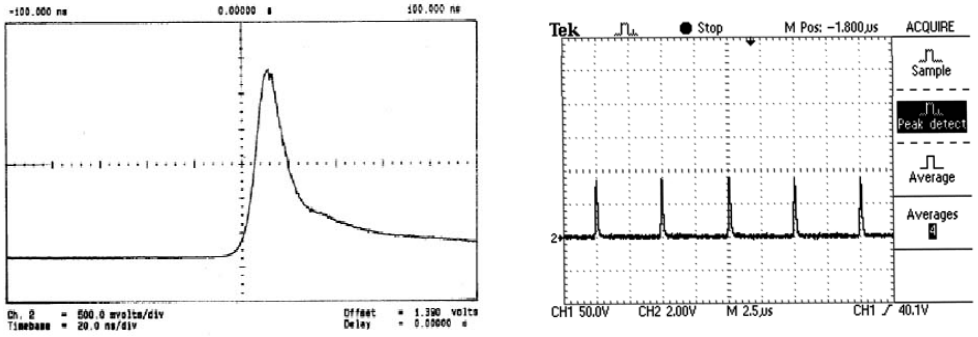

Figure 20. Pulse width and repetition rate of a Q-switch made from an OptoCeramic PMN-PT.

3.6. Tunable optical filters

Wavelength tunable filters would be very useful for a wide range of applications, such as telecommunications, lidar and ladar, remote sensing, and analyzing. Commercially available optical filters include mechanically tuned Fabry-Perot etalon, liquid-crystal filters and acousto-optic filters. Some of these tunable filters are heavy and bulky,

while others are slow and unreliable. Electro-optic based devices are intrinsically fast, a critical requirement for current and future photonic systems. There are two kinds of EO tunable filters that have been widely used: Tunable Lyot Filter (TLF) and Tunable Fabry-Perot filter (TFPF). TLF has wider and more stable tuning range but, however, higher optical loss since it requires polarizers. TFPF usually has narrower bandwidth, larger aperture, better transmission, but narrower tuning range. They can be used separately or jointly. Using OptoCeramic PMN-PT as the dynamic tuning component, we fabricated both TLF and TFPF.

Shown in Figure 20(a) is a 4-stage TLF where each stage consists of a polarizer and a tunable waveplate of PMN-PT. The tunable waveplates are in harmonic lengths. Figure 20(b) shows a picture of a fiber-version 4-stage TLF (uncovered) with driving circuit. Characteristics of the TLF are shown in Figure 21, where 3 stages were powered. The transmitted band position is determined by the total birefringence and the tuning is realized by voltage-induced birefringence. That is, when the birefringence varies, the peak wavelength moves.

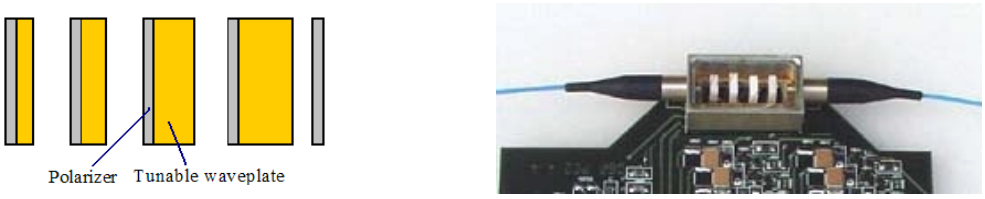

(a) (b)

Figure 20. (a) A schematic design of TFL, (b) A fiber-version 4-stage TLF (uncovered) with driving circuit.

The TFPF is constructed by sandwiching an OptoCeramic, with both sides coated with transparent electrodes, between two partial reflection mirrors. We used ITO as the transparent electrode while SiO_2/TiO_2 multiplayer as the dielectric mirror. In order to operate the TFPF in the entire specified wavelength range, the tunability of a TFPF must be such that the tuning range of each transmission peak is greater than or equal to the FSR of the etalon so that the adjacent peak could continue cover the next wavelength window by a range of another FSR.

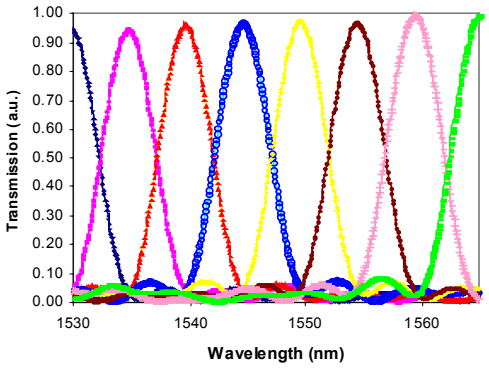

Figure 21. TLF responses when 3 stages were powered.

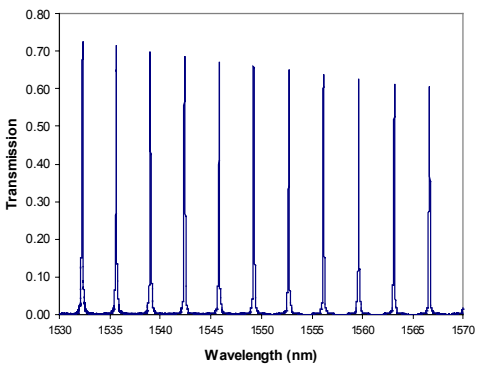

Figure 22. Ttransmission spectrum of a TFPF.

Figure 22 shows the transmission spectrum of a TFPF (150-μm thick) characterized by using an Ando 6317 optical spectra analyzer. The finesse was determined to be 33, the insertion loss (IL) 1.6 dB, and the FSR 3.5 nm, respectively. About 2.1 nm wavelength shift was obtained by applying a 1.0 V/μm electrical field, which is very close to the estimated value (2.3 nm) according to the measured Δn. A tuning range of 6 nm was demonstrated by

applying higher electric field. The tuning speed was measured from another setup on similar OptoCeramic structure to be about 500 ns.

By combining two TFPFs with slightly different FSRs, the tuning can be very adaptive and efficient (lower voltage required). For instance, when a transmission peak of TFPF 1 coincides with a transmission peak of TFPF 2, light of this wavelength is transmitted. Shown in Figure 23 are the experimental results of tuning range of a dual-cavity TFPF when only one TFPF is tuned. With moderate electric field, the FSR shown in Figure 23 is about 70 nm. When both TFPFs are tuned, the wavelength selection range is wider.

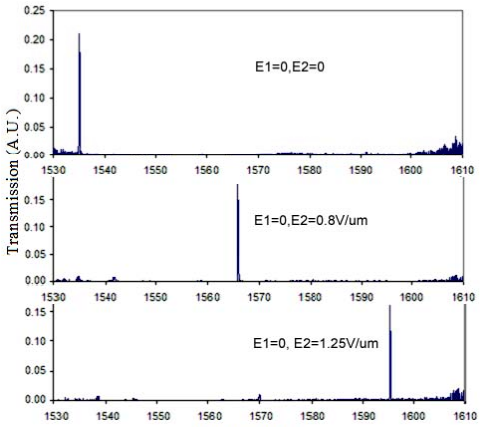

Figure 23. Measured outputs of a composite TFPF with different applied voltages.

4. CONCLUSIONS

We have demonstrated the superior performance of OptoCeramic materials in terms of high electro-optic effect, wide transmission wavelength range, low optical loss, fast response speed, and ceramic ruggedness. A variety of high performance devices made from the OptoCeramic materials have been developed and demonstrated, with some of them representing the current state-of-the-art. This materials family and its corresponding electro-optic components will have great applications in telecommunications, instrumentations, and many other areas where various optical parameters, such as intensity, polarization, phase, and modulation, need to be managed precisely and reliably.

REFERENCES

1 G.H. Haertling and C.E. Land, "Hot-pressed (Pb,La)(Zr,Ti,)O3 ferroelectric ceramics for electrooptic applications," *J. Am. Ceram. Soc.*, **51** 1 (1971).

2 K.K. Li, *et al.*, "Electro-optic ceramic material and device, PMN-PT" US Patent Application 10/139857, 5/6/02.

3 K.K. Li, *et al.*, "Electro-optic ceramic material and device, PZN-PT" US Patent Number 6746618, 2004.

4. G.H. Haertling, *Ferroelectrics,* **75** 25 (1987).

5 T. R. Shrout and J. F. Fielding, Jr., *IEEE Ultrasonics Symp.,* 711 (1990).

6 C. D. Poole and R. E. Wagner, *Electronics Letters,* **22** 1029 (1986).

7 G. Keiser, "A review of WDM technology and applications," *Optical Fiber Tech.* **5** 3 (1999).

8 X. Yin, S. Zhang, and J. Wang, "Mutual action of optical activity and electro-optic effect and its influence on the electro-optic Q-switch" *Optical Review* **11** 328-31 (2004).

9 Y.H. Chen and Y.C. Huang, "Actively Q-switched Nd:YVO4 laser using an electro-optic periodically poled lithium niobate crystal as a laser Q-switch," *Opt Lett.* **28** 1460 (2003).

10 Maris Ozolinsh, *et al.*, "Q-Switching of Er:YAG (2.9μm) solid-state laser by PLZT electrooptic modulator," *IEEE J. of Quant. Electronics* **33** 10 (1997).

11 G. Wang, H. Jiang, and J. Zhao, "Low voltage electro-optic Q-switching of 1.06 um microlasers by PLZT," *CLEO'98* 485 (1998).